

# Gamma-Ray Burst Afterglow: Polarization and Analytic Light Curves

Andrei Gruzinov & Eli Waxman

Institute for Advanced Study, School of Natural Sciences, Princeton, NJ 08540

## ABSTRACT

GRB afterglow polarization is discussed. We find an observable, up to  $\sim 10\%$ , polarization, if the magnetic field coherence length grows at about the speed of light after the field is generated at the shock front. Detection of a polarized afterglow would show that collisionless ultrarelativistic shocks can generate strong large scale magnetic fields and confirm the synchrotron afterglow model. Non-detection, at  $\sim 1\%$  level, would imply that either the synchrotron emission model is incorrect, or that strong magnetic fields, after they are generated in the shock, somehow manage to stay un-dissipated at “microscopic”, skin depth, scales. Analytic lightcurves of synchrotron emission from an ultrarelativistic self-similar blast wave are obtained for an arbitrary electron distribution function, taking into account the effects of synchrotron cooling. The peak synchrotron flux and the flux at frequencies much smaller than the peak frequency are insensitive to the details of the electron distribution function; hence their observational determination would provide strong constraints on blast wave parameters.

*Subject headings:* gamma rays: bursts – magnetic fields – shocks

## 1. Introduction

X-ray, optical and radio emission following gamma-ray bursts (GRBs) are in broad agreement with models based on relativistic blast waves at cosmological distances (Waxman 1997a, Wijers, Rees & Mészáros 1997, Vietri 1997b, Reichart 1997, Katz & Piran 1997, Sari, Piran, & Narayan 1998). In these models, the energy released by an explosion,  $\sim 10^{52}$ erg, is converted to kinetic energy of a thin baryon shell expanding at ultra-relativistic speed. After producing the GRB, the shell impacts on surrounding gas, driving an ultra-relativistic shock into the ambient medium. In what follows, we refer to the surrounding gas as interstellar medium (ISM) gas, although the gas need not necessarily be inter-stellar. The expanding shock continuously heats fresh gas and accelerates relativistic electrons, which produce the observed afterglow radiation through synchrotron emission (Paczynski & Rhoads 1993, Mészáros & Rees 1997, Vietri 1997a).

To match the observations, the magnetic field behind the shock has to be  $\sim 10\%$  of equipartition with the shock-heated, compressed ISM. What is the origin of this field? The

shock-compressed ISM field is many orders of magnitude smaller than needed. The magnetic field frozen into the initial GRB fireball loses strength by the time the afterglow stage begins, and it is in a wrong place anyway. During the afterglow, the decompressed GRB field is located far behind the shock, while most of the energy is in the recently shocked ISM. Therefore, the magnetic field most likely must be generated in and by the blast wave. If the coherence length of the generated field is comparable to the thickness of the blast wave, the radiation will be polarized. An  $\sim 10\%$  degree of polarization is expected. This is significantly smaller than the maximal synchrotron polarization,  $\sim 70\%$ , because the emitting region is thin and broad; it must be covered by  $\sim 100$  mutually incoherent patches of magnetic field.

In a paper on microlensing of GRB afterglows, Loeb & Perna (1998) have mentioned the possibility that the afterglows are polarized. Here we estimate the degree of polarization (§4). This paper also provides (§3) exact analytic afterglow lightcurves for an arbitrary electron distribution function, including the effects of electron cooling. In §2 we describe the underlying model assumptions. We discuss the implications of our results to afterglow observations in §5. Most of the details of our derivations are given in appendices A–E.

## 2. The blast wave model

A strong blast wave is fully specified by two parameters: the blast wave energy  $E = 10^{52} E_{52}$  erg, and the ISM density  $n_i = 1 n_1 \text{ cm}^{-3}$ . With sufficient accuracy, the unshocked ISM may be taken to be cold unmagnetized hydrogen. To calculate the synchrotron emission we need to know the fraction of energy in magnetic fields  $\xi_B$ , and in electrons  $\xi_e$ , and the shape of the electron distribution function (a function  $f_e(z)$  with first two moments equal to 1). We include  $\xi_B$ ,  $\xi_e$ , and  $f_e(z)$  in the list of independent parameters. In principle, these are determined by the blast wave energy and the ISM density, but a theory of strong collisionless shocks is not available (Sagdeev 1966, Krall 1997).

The plasma flow in the shocked ISM is assumed to be described by the Blandford-McKee (Blandford & McKee 1976) self-similar solution. The Lorentz factor of the shock wave  $\Gamma$ , the Lorentz factor of the flow  $\gamma$ , the proper energy density  $e$ , and the proper number density  $n$  for all space-time points in the shocked plasma are given in Appendix A.

We assume that magnetic fields and electrons are described by simple scalings. The magnetic field is  $B^2/8\pi = \xi_B e$ , and  $\xi_B$  is the same in all space-time points. The electron distribution function in the local rest frame has the same shape in all space-time points on the shock front, after the shock passage it evolves by adiabatic and synchrotron cooling. At the shock front, the mean energy of an electron in the local rest frame is  $\gamma_e m_e c^2 = \xi_e e/n$ , and  $\xi_e$  is constant. The shape of the electron distribution function is not specified at this point. We include  $f_e(z)$  into the definition of the synchrotron emission function  $F$ . The synchrotron power per unit frequency per

electron emitted in the local rest frame is

$$P(\omega) = \frac{\sqrt{3}}{2\pi} \frac{e^3 B}{m_e c^2} F\left(\frac{\omega}{\omega_c}\right), \quad (1)$$

$$\omega_c = \frac{3\gamma_e^2 e B}{2m_e c}, \quad (2)$$

but  $F$  is *not* the standard dimensionless synchrotron emission function given in Rybicki & Lightman (1979).  $F$  depends on the shape of the electron distribution function (B7).

Given the set of blast wave parameters, we will measure time, frequency, and spectral luminosity (energy per time per frequency) in units of

$$T = c^{-1} \left( \frac{17}{8\pi} \frac{E}{n_i m_p c^2} \right)^{1/3} = 5.5 \times 10^7 \left( \frac{E_{52}}{n_1} \right)^{1/3} \text{ s}, \quad (3)$$

$$\omega_0 \equiv 3\sqrt{\pi} \left( \frac{m_p}{m_e} \right)^{5/2} \frac{c}{r_e} \xi_B^{1/2} \xi_e^2 (n_i r_e^3)^{1/2} = 3.9 \times 10^{10} \left( \frac{\xi_e}{0.1} \right)^2 \left( \frac{\xi_B}{0.1} \right)^{1/2} n_1^{1/2} \text{ s}^{-1}, \quad (4)$$

$$E_0 \equiv \frac{17}{2\sqrt{6\pi}} \left( \frac{m_e}{m_p} \right)^{1/2} \xi_B^{1/2} (n_i r_e^3)^{1/2} E = 2.2 \times 10^{31} \left( \frac{\xi_B}{0.1} \right)^{1/2} n_1^{1/2} E_{52} \text{ erg}. \quad (5)$$

The formal origin of these units is explained in Appendices A, B. Their physical meaning is illustrated by the following order of magnitude statement. At observed time  $t_o/T = 1$ , the blast wave slows down to Lorentz factor 2; it radiates at frequency  $\omega/\omega_0 = 1$ , with spectral luminosity  $L/E_0 = 1$ . Our analysis is restricted to the ultrarelativistic stage, that is to dimensionless observed times  $t_o \ll 1$ .

### 3. Lightcurves

We first calculate in §3.1 synchrotron emission of the blast wave neglecting radiative cooling of electrons, i.e. assuming that the shape  $f_e(z)$  is the same in the entire shocked plasma. In §3.2 we relax this assumption:  $f_e(z)$  is determined at the shock front and evolves by synchrotron and adiabatic cooling thereafter.

Our analytic lightcurves are exact under the following assumptions: (i) The blast-wave hydrodynamics is described by the Blandford-McKee self-similar solution (Blandford & McKee 1976); (ii) The magnetic field energy density is a fixed fraction of the total energy density, independent of space and time; (iii) The electron distribution function is determined at the shock front and evolves afterwards only through adiabatic and synchrotron cooling. Granot, Piran, & Sari 1998 numerically derived exact lightcurves for power-law electron distribution, under the assumptions described above and neglecting electron cooling. It should be emphasized that since a theory of strong collisionless shocks is not available at present, none of the above assumptions can be justified. Thus, the numerical values (e.g. of the peak flux and peak frequency as function of

time) derived here under these assumptions are not necessarily more accurate than those obtained by order of magnitude estimates (e.g. Waxman 1997b, Sari, Piran, & Narayan 1998, Wijers & Galama 1998).

The exact analytic lightcurves are useful because they allow us to determine which afterglow characteristics are strongly dependent on the details of the electron distribution function, and which are insensitive to these details and depend mainly on the global blast wave parameters (i.e. the blast wave energy, the ambient medium density, and the energy fractions carried by electrons and magnetic fields).

### 3.1. Adiabatic Lightcurve

In Appendix B, we derive an expression for the spectral luminosity, neglecting synchrotron cooling of electrons. At observed time  $t_o$  after the gamma-burst, at frequency  $\omega$ , distant observer (with negligible redshift) infers a selfsimilar narrow-band luminosity of the blast wave  $L_\omega(t_o) = L_A(\omega t_o^{3/2})$ , where

$$L_A(\omega) = 48 \int_0^1 da \, a^3 (1 + 7a^2)^{-2} F[2a(1 + 7a^2)\omega]. \quad (6)$$

We show the lightcurves in Fig.1. The three curves correspond to different doubly normalized electron distribution functions:

1. Power law, index  $p = 2.4$ :  $f_e = f_P = 31.2z^2(1 + 122z^{p+2})^{-1}$
2. Maxwellian:  $f_e = f_M = 13.5z^2e^{-3z}$
3. Mixed:  $f_e = 0.7f_M + 0.3f_P$

Note, that our “power-law” distribution, for which  $f_e \propto z^{-p}$  for  $z \gg 1$ , includes a low energy tail,  $f_e \sim z^2$  for  $z \ll 1$ . We believe the inclusion of such a “thermal” low energy tail is more realistic than assuming a sharp cutoff of the electron distribution below a certain minimum  $z$  value.

### 3.2. Lightcurve with synchrotron cooling

At early times or at high frequencies, synchrotron cooling of the electron distribution function will have a noticeable effect on the lightcurve. We calculate the nonadiabatic lightcurve,  $L_\omega(t_o) = L_{NA}(\omega, t_o)$  in Appendix C, neglecting effects of cooling on the blast wave propagation:

$$L_{NA}(\omega, t_o) = 192 \int_0^1 dy \, y^3 \int_0^1 da \, a^3 (1 + 7a^2)^{-2} \int dz_0 \, f_e(z_0) F_0[2a(1 + 7a^2)\omega t_o^{3/2} z^{-2}], \quad (7)$$

where

$$z^{-1} = z_0^{-1} + A(8t_o)^{-1/2} a^{-1} y^{-2} (1 - y^{19/6}), \quad (8)$$

and

$$A = \frac{8}{19} \left( \frac{m_p}{m_e} \right)^2 \sigma_T c T n_i \xi_B \xi_e = 1.6 \times 10^{-2} \left( \frac{\xi_e}{0.1} \right) \left( \frac{\xi_B}{0.1} \right) E_{52}^{1/3} n_1^{2/3}. \quad (9)$$

Scaled spectra at different observed time  $t_o$  are shown in Fig. 2 for the power-law (and in Fig. 3 for the mixed) electron distribution function of §3.1 and  $A = 0.01$ . At high frequencies, eqs. (7), (8) predict a power-law luminosity  $L \propto \omega^{-p/2}$  for an electron distribution function with a power-law tail of index  $p$ .

### 3.3. Observables

From Eqs. (3)-(5) and Figs. 2, 3, an afterglow at redshift  $z_b$ , observed  $t_{\text{day}}$  days after the  $\gamma$ -burst, will show maximal flux at a frequency

$$\nu_m \sim 3 \times 10^{12} \frac{\sqrt{1+z_b}}{\sqrt{2}} \left( \frac{\xi_e}{0.1} \right)^2 \left( \frac{\xi_B}{0.1} \right)^{1/2} E_{52}^{1/2} t_{\text{day}}^{-3/2} \text{Hz}. \quad (10)$$

The maximal flux does not depend on the time of observation. In a flat universe with Hubble constant  $H_0 = 75 \text{ km/s/Mpc}$ ,

$$F_{\nu m} = 4 \left( \frac{\sqrt{1+z_b}-1}{\sqrt{2}-1} \right)^{-2} \left( \frac{\xi_B}{0.1} \right)^{1/2} n_1^{1/2} E_{52} \text{mJy}. \quad (11)$$

As seen in Figs. 1, 2, 3, the peak flux  $F_{\nu m}$  is robust, i.e. it is independent of the details of the electron distribution function. The flux below the peak is also robust, and for  $\nu \ll \nu_m$  it is given by

$$F_\nu = 0.6 \left( \frac{\sqrt{1+z_b}-1}{\sqrt{2}-1} \right)^{-2} \left( \frac{1+z_b}{2} \right)^{-1/6} \left( \frac{\xi_e}{0.1} \right)^{-2/3} \left( \frac{\xi_B}{0.1} \right)^{1/3} n_1^{1/2} E_{52}^{5/6} t_{\text{day}}^{1/2} \nu_{\text{GHz}}^{1/3} \text{mJy}. \quad (12)$$

The peak frequency  $\nu_m$  is model-dependent, and may differ by an order of magnitude between different electron distribution functions with similar  $\xi_e$ . The spectral shape (equivalently the time profile) above the peak is also strongly dependent on the details of the electron distribution function.

## 4. Polarization

Synchrotron radiation is highly polarized (Ginzburg 1989), but for this polarization to be measurable in an unresolved source, the magnetic field coherence length should be comparable to the source size. Here we show that GRB afterglows might be polarized. An  $\sim 10\%$  polarization

seems to be an upper bound, corresponding to a coherence length that grows at about the speed of light after the field is generated at the shock front.

Qualitatively, our polarization analysis can be summarized as follows. Suppose that the magnetic field coherence length in the local rest frame is  $l \sim c\tau$ , where  $\tau$  is the proper time after the shock. The extension of the emitting region transverse to the line of site is  $\sim 5c\tau$ . There are  $\sim 50$  coherent patches. The degree of polarization is  $\sim 60\%/\sqrt{50} \sim 10\%$ . If the coherence length is smaller than the proper time,  $l \sim \epsilon c\tau$ ,  $\epsilon < 1$ , the degree of polarization is decreased to

$$\Pi \sim 10\epsilon^{3/2} \%. \quad (13)$$

The degree and direction of polarization should depend on time, the polarization coherence time should be  $\sim \epsilon t_o$ .

#### 4.1. Magnetic field generated by a relativistic collisionless shock

As far as we know, magnetic field generation in collisionless shocks is not understood. It seems possible that, at the shock front, Weibel instability generates near equipartition ( $\xi_B \sim 0.1$ ) small scale ( $\sim$  skin depth  $\delta$ , here  $\delta = c/\omega_p$ ,  $\omega_p^2 \sim ne^2/\gamma_p m_p \lesssim ne^2/\gamma_e m_e$ ) magnetic fields. By magnetic moment conservation, electrons are accelerated to near equipartition energies (relativistic version of Sagdeev 1966, Kazimura et. al. 1998). The ultimate fate of the field many skin depth behind the shock front is not clear. What happens to the magnetic field coherence length  $l$ , and to the magnitude  $B$  at a distance  $\Delta \gg \delta$  behind the shock front? Three scenarios seem to make sense:

1. The generated field dies out after finishing its job of isotropizing the plasma and bringing it to a state given by the shock jump conditions.
2. The magnitude stays at about equipartition, the coherence length stays at about the skin depth.
3. The magnitude stays at about equipartition, the coherence length grows as  $l \sim \Delta$ .

Scenario 1 is not consistent with the synchrotron emission model for the afterglow, because too little synchrotron radiation is produced by a skin-deep shell with strong magnetic fields. Scenario 2 means unpolarized radiation. We will evaluate the degree of polarization for scenario 3.

#### 4.2. Coherent patch

Assume that two events in the shocked ISM belong to the same coherent patch if the difference in their proper times elapsed after the shock passage  $\delta\tau$ , and their spatial separation transverse to the line of site  $\delta h$  are small:

$$\delta\tau < \epsilon\tau, \quad (14)$$

$$\delta h < \epsilon_h c\tau, \quad (15)$$

$\epsilon_\tau, \epsilon_h < 1$ ,  $\tau$  is the averaged proper time since the shock. By the proper time of an event in the shocked ISM we mean the proper time after the shock of a fluid particle at this event.

### 4.3. Degree of Polarization

As shown in Appendix D, for the emission event with observed time  $t_o$ , the proper time  $\tau$  (in units of  $T$ ) and the transverse distance (in units of  $cT$ ) are

$$\tau = 1.15 t_o^{5/8} a^{5/4} y^{1/4} (1 - y^{9/4}), \quad (16)$$

$$h = 1.83 t_o^{5/8} a^{1/4} (1 - a^2)^{1/2} y^{1/4}. \quad (17)$$

Here the meaning of dimensionless variables  $a$ ,  $y$  is unimportant, what matters is that the luminosity is given by the integral (B20) over  $a$  and  $y$ :

$$L(\omega) = 192 \int_0^1 dy y^3 \int_0^1 da a^3 (1 + 7a^2)^{-2} F[2a(1 + 7a^2)\omega]. \quad (18)$$

Now we can separate the full luminosity (18) into coherent parts according to the criterion (14),(15). This gives, approximately, the degree of polarization. By numerical simulations (Appendix E),

$$\Pi \sim 10 \epsilon_h \epsilon_\tau^{1/2} \%. \quad (19)$$

## 5. Summary of results

### 5.1. Lightcurves

We have derived simple, exact analytic afterglow lightcurves for an arbitrary electron distribution function, including the effects of electron synchrotron cooling, Eq. (7), and in the limit where synchrotron cooling is negligible, Eq. (6). Our lightcurves are exact under the following assumptions: (i) The blast-wave hydrodynamics is described by the Blandford-McKee self-similar solution (Blandford & McKee 1976); (ii) The magnetic field energy density is a fixed fraction of the total energy density, independent of space and time; (iii) The electron distribution function is determined at the shock front and evolves afterwards only through adiabatic and synchrotron cooling.

We have shown, see. Fig. 1, 2, 3, that the peak synchrotron flux, Eq. (11), and the synchrotron flux at frequencies well below the peak flux, Eq. (12), are insensitive to the details of the electron distribution function. Since the peak flux is also insensitive to the details of the blast wave hydrodynamic profiles (Fig. 1 in Waxman 1997c), the peak flux and the flux at

frequencies well below the peak depend mainly on the global blast wave parameters: blast wave energy, ambient medium density, magnetic field and electron energy fractions [cf. Eqs. (11,12)]. Observational determination of these fluxes would therefore provide strong constraints on blast wave parameters. The numerical value of the peak flux derived here, Eq. (11), is similar to that derived in Granot, Piran, & Sari 1998, within a factor  $\sim 3$  of the values given in Waxman 1997b and Wijers & Galama 1998, and a factor  $\sim 10$  smaller than given in Sari, Piran, & Narayan 1998. The discrepancy with Sari, Piran, & Narayan 1998 is mainly due to the fact that it is assumed by these authors that the spectral width of the observed spectrum at fixed time is determined mainly by the intrinsic spectral width of synchrotron emission, while the actual width is significantly larger and dominated by contribution to the observed spectrum at given time from different space-time points with different plasma conditions.

The peak frequency and spectral shape at frequencies above the peak are strongly dependent on details of the electron distribution function, see Figs. 1, 2, 3. Furthermore, the peak frequency is also strongly dependent on the details of the blast wave hydrodynamic profiles (Fig. 1 in Waxman 1997c). This, and the fact that the spectral peak is flat, imply that observational determination of the peak frequency and of spectral features above the peak at a given time can not be used directly to constrain global blast wave parameters. These features would mostly provide information on the electron distribution function. The numeric value of the peak frequency derived here, Eq. (10), is within a factor  $\sim 3$  of the values given in Sari, Piran, & Narayan 1998, Granot, Piran, & Sari 1998 and Wijers & Galama 1998, and a factor  $\sim 10$  smaller than given in Waxman 1997b. The discrepancy with Waxman 1997b is due mainly to the fact that it is assumed in Waxman 1997b that the spectral peak is close to the synchrotron frequency of electrons with average Lorentz factor, while the actual peak is closer to the synchrotron frequency of electrons near the peak of the electron distribution function.

The break frequency (the frequency where the high-frequency spectrum changes the slope from  $(p-1)/2$  to  $p/2$  due to synchrotron cooling) is not prominent. The transition to the  $p/2$  slope occurs in a manner that strongly depends on the details of the electron distribution function.

## 5.2. Polarization

If the observed afterglows are indeed synchrotron emission from ultrarelativistic blast waves propagating into ISM, the magnetic field needed to account for the emission must be generated by the blast wave. If the coherence length of the generated field grows at about the speed of light after the field was generated at the shock front, afterglows should be noticeably polarized.

We thank John Bahcall for a discussion that initiated this study. Our work was supported by NSF PHY-9513835. EW was also supported by the W. M. Keck Foundation.



### A. Ultrarelativistic blast wave.

The Blandford & McKee (1976) solution can be described as follows.

Let  $(t, r, \theta)$  be the space-time coordinates in the blast frame,  $\theta$  is the polar angle which is assumed to be small, with  $\theta = 0$  in the observer direction. Let  $E$  be the energy of the blast wave, and  $n_i$  the unshocked ISM number density,  $c = 1$ . The shock front propagates into the ISM with a Lorentz factor  $\Gamma$  that decreases with time according to

$$\Gamma^2 t^3 = \frac{17}{8\pi} \frac{E}{n_i m_p} \equiv T^3. \quad (\text{A1})$$

Define a similarity variable

$$\chi \equiv 8\Gamma^2 \left(1 - \frac{r}{t}\right). \quad (\text{A2})$$

The shocked region is  $\chi > 1$ , and the fluid flow in the shocked region is given by

$$\gamma^2 = \frac{1}{2} \Gamma^2 \chi^{-1}, \quad (\text{A3})$$

$$e = 2\Gamma^2 \chi^{-17/12} n_i m_p, \quad (\text{A4})$$

$$n = 2\sqrt{2}\Gamma \chi^{-5/4} n_i. \quad (\text{A5})$$

Here  $\gamma$  is the Lorentz factor of the flow,  $e$  is the proper energy density,  $n$  is the proper number density.

In Appendix B, we use  $(\Gamma, \gamma, t_{\text{obs}})$  as independent variables instead of  $(t, r, \theta)$ . Here  $t_{\text{obs}}$  is the time at which a photon emitted at  $(t, r, \theta)$  is observed; with sufficient accuracy,

$$t_{\text{obs}} = t - r + r \frac{\theta^2}{2} = t - r + t \frac{\theta^2}{2}. \quad (\text{A6})$$

The coordinate transformation is (old coordinates in terms of new coordinates)

$$t = T\Gamma^{-2/3}, \quad (\text{A7})$$

$$r = \left(1 - \frac{1}{16\gamma^2}\right)t = \left(1 - \frac{1}{16\gamma^2}\right)T\Gamma^{-2/3}, \quad (\text{A8})$$

$$\frac{\theta^2}{2} = \frac{t_{\text{obs}}}{t} - \frac{1}{16\gamma^2} = \frac{t_{\text{obs}}}{T}\Gamma^{2/3} - \frac{1}{16\gamma^2}. \quad (\text{A9})$$

From (A3)

$$\chi = \frac{\Gamma^2}{2\gamma^2}. \quad (\text{A10})$$

With  $\chi$  from (A10), expressions (A4), (A5) give the dependent quantities, energy density and density, in terms of new independent variables. In new coordinates, the space-time domain of the shocked fluid ( $t > 0$ ,  $\chi > 1$ ,  $\theta > 0$ ) is given by

$$\infty > t_{\text{obs}} > 0, \quad (\text{A11})$$

$$\infty > \Gamma > \left( \frac{8t_{\text{obs}}}{T} \right)^{-3/8}, \quad (\text{A12})$$

$$\frac{\Gamma}{\sqrt{2}} > \gamma > \frac{1}{4} \left( \frac{t_{\text{obs}}}{T} \right)^{-1/2} \Gamma^{-1/3}. \quad (\text{A13})$$

## B. Lightcurve

Here we calculate the lightcurve of synchrotron emission from an ultrarelativistic blast wave. The physical assumptions of the model are discussed in the main text.

It is convenient to start from the following expression for the total emitted energy

$$E_r = \int r^2 dr \int 2\pi\theta d\theta \int dt n \int d\omega' P(\omega', \gamma_e, B) \frac{\omega}{\omega'} \frac{d\Omega'}{d\Omega}. \quad (\text{B1})$$

The factors in (B1) are:

1. Total number of emitting electrons at a given time

$$\int r^2 dr 2\pi\theta d\theta \gamma n. \quad (\text{B2})$$

2. Total energy emitted by one electron

$$\int \frac{dt}{\gamma} \int d\omega' P(\omega', \gamma_e, B) \frac{\omega}{\omega'}, \quad (\text{B3})$$

where  $\omega$  is the photon frequency in the burst frame, and  $\omega'$  is the frequency in the local rest frame,

$$\omega' = \frac{1 + \gamma^2 \theta^2}{2\gamma} \omega. \quad (\text{B4})$$

$P(\omega', \gamma_e, B)$  is the synchrotron radiation spectral power in the local rest frame emitted at the frequency  $\omega'$ , by one electron from a distribution with a mean Lorentz factor  $\gamma_e$ , in the magnetic field  $B$ . It is given by (Rybicki & Lightman 1979)

$$P(\omega', \gamma_e, B) = \frac{\sqrt{3}e^3}{2\pi m_e c^2} B F\left(\frac{\omega'}{\omega_c}\right), \quad (\text{B5})$$

$$\omega_c(\gamma_e, B) = \frac{3e}{2m_e c} B \gamma_e^2, \quad (\text{B6})$$

The dependence of emission on the mean Lorentz factor of electrons is shown explicitly. The dependence on the detailed distribution function of electrons is hidden in the definition of the synchrotron emission function  $F(x)$ . Namely, we define

$$F(x) = \int dz f_e(z) F_0\left(\frac{x}{z^2}\right), \quad (\text{B7})$$

with  $F_0(x)$  being the standard synchrotron emission function

$$F_0(x) \equiv x \int_x^\infty d\xi K_{5/3}(\xi). \quad (\text{B8})$$

In (B7), the normalized electron distribution function  $f_e$  is defined by the following expression for the probability for the electron to have a Lorentz factor  $\gamma_{el}$

$$\frac{d\text{Probability}}{d\gamma_{el}} = \frac{1}{\gamma_e} f_e \left( \frac{\gamma_{el}}{\gamma_e} \right). \quad (\text{B9})$$

3. The last factor in (B1) is the ratio of infinitesimal solid angles in the local rest and blast frames:

$$\frac{d\Omega'}{d\Omega} = \frac{4\gamma^2}{(1 + \gamma^2\theta^2)^2}. \quad (\text{B10})$$

We assume that magnetic fields and electrons take up a fixed fraction of the proper energy density  $e(r, t)$ :

$$\frac{B^2}{8\pi} = \xi_B e, \quad (\text{B11})$$

and

$$\gamma_e n m_e c^2 = \xi_e e. \quad (\text{B12})$$

We also assume that the normalized electron distribution function  $f_e(z)$  in the shocked ISM is fixed. These assumptions might be approximately correct when synchrotron cooling becomes unimportant at later stages of the afterglow.

We use the Blandford & McKee (1976) selfsimilar solution for the Lorentz factor  $\gamma$ , density  $n$ , and energy density  $e$ , and change the independent variables in (B1) from  $(t, r, \theta, \omega')$  to  $(\Gamma, \gamma, t_{\text{obs}}, \omega)$ . Using Appendix A, we get

$$E_r = \frac{17}{48} \frac{E}{n_i m_p c^2} \int_0^\infty d\omega \int_0^\infty dt_{\text{obs}} \int_{(8t_{\text{obs}}/T)^{-3/8}}^\infty d\Gamma \Gamma^{-3} \int_{(t_{\text{obs}}/T)^{-1/2}\Gamma^{-1/3}/4}^{\Gamma/\sqrt{2}} d\gamma \gamma^{-3} n D^2 P(D^{-1}\omega, \gamma_e, B). \quad (\text{B13})$$

Here  $D$  is the ‘‘Doppler factor’’

$$D = \frac{2\gamma}{1 + \gamma^2\theta^2} = 2\gamma \left( \frac{7}{8} + 2\frac{t_{\text{obs}}}{T} \Gamma^{2/3} \gamma^2 \right)^{-1}, \quad (\text{B14})$$

and  $T$  is the characteristic time of the blast wave introduced in Appendix A.

The spectral lightcurve is defined as luminosity per unit frequency:

$$L_\omega(t_{\text{obs}}) \equiv \frac{dE_r}{dt_{\text{obs}} d\omega}. \quad (\text{B15})$$

From (A14),

$$L_\omega(t_{\text{obs}}) = \frac{17}{48} \frac{E}{n_i m_p c^2} \int_{(8t_{\text{obs}}/T)^{-3/8}}^{\infty} d\Gamma \Gamma^{-3} \int_{(t_{\text{obs}}/T)^{-1/2} \Gamma^{-1/3/4}}^{\Gamma/\sqrt{2}} d\gamma \gamma^{-3} n D^2 P(D^{-1}\omega, \gamma_e, B). \quad (\text{B16})$$

Now we use expression (B5) for the synchrotron power  $P$ , (B11) and (B12) for  $B$  and  $\gamma_e$ , (A4), (A5), (A10) for  $e$  and  $n$ . Also, from now on we will denote by  $t_o$  the observed time measured in units of  $T$ . We also define the frequency and spectral luminosity units, equations (4),(5). These are devised to get rid of constant factors in the resulting expression for the luminosity. We denote the frequency  $\omega$  in units of  $\omega_0$  by  $\omega$ , and the spectral luminosity  $L_\omega(t_{\text{obs}})$  in units of  $E_0$  by  $L_\omega(t_o)$ . Then (B16) takes the following form

$$L_\omega(t_o) = \int_{(8t_o)^{-3/8}}^{\infty} d\Gamma \Gamma^{-1} \int_{t_o^{-1/2} \Gamma^{-1/3/4}}^{\Gamma/\sqrt{2}} d\gamma \gamma^{-3} \left( \frac{\Gamma^2}{2\gamma^2} \right)^{-47/24} D^2 F[ D^{-1}\omega \Gamma^{-3} \left( \frac{\Gamma^2}{2\gamma^2} \right)^{25/24} ]. \quad (\text{B17})$$

Define new integration variables  $x$  and  $y$ :  $\gamma \equiv (\Gamma/\sqrt{2})y$ ,  $\Gamma \equiv (8t_o)^{-3/8}x^{-3/4}$ . We obtain a selfsimilar spectral lightcurve

$$L_\omega(t_o) = L_A(\omega t_o^{3/2}). \quad (\text{B18})$$

Here

$$L_A(\omega) = 192 \int_0^1 dx x^{-1} \int_x^1 dy y^{35/12} (7 + \frac{y^2}{x^2})^{-2} F[ 2x^3 y^{-37/12} (7 + \frac{y^2}{x^2}) \omega ]. \quad (\text{B19})$$

With only an  $\sim 2\%$  error in the resulting luminosity, we can replace the indices 35/12 and 37/12 by 3, and get a simpler expression

$$L_A(\omega) = 192 \int_0^1 dy y^3 \int_0^1 da a^3 (1 + 7a^2)^{-2} F[ 2a(1 + 7a^2) \omega ], \quad (\text{B20})$$

where  $a \equiv x/y$ . From (B20), the adiabatic lightcurve is

$$L_A(\omega) = 48 \int_0^1 da a^3 (1 + 7a^2)^{-2} F[ 2a(1 + 7a^2) \omega ]. \quad (\text{B21})$$

### C. Synchrotron cooling

Synchrotron plus adiabatic cooling of an electron with Lorentz factor  $\gamma_{el}$  is described by

$$\frac{d\gamma_{el}}{d\tau} = \frac{1}{3} \frac{\gamma_{el}}{n} \frac{dn}{d\tau} - \frac{4}{3} \sigma_{Tc} \frac{B^2}{8\pi m_e c^2} \gamma_{el}^2, \quad (\text{C1})$$

where  $\tau$  is the proper time of the fluid element at the electron's location. We have  $d\tau = dt/\gamma$ . From (A5),  $d \ln n = d \ln \Gamma - (5/4)d \ln \chi$ . From (D8),  $d \ln \chi = 4d \ln t$ . Then

$$\frac{d\gamma_{el}}{dn} = \frac{1}{3} \frac{\gamma_{el}}{n} - \frac{4}{3} \sigma_{Tc} \frac{B^2}{8\pi m_e c^2} \gamma_{el}^2 \frac{1}{\gamma n} \left( \frac{d \ln \Gamma}{dt} - \frac{5}{t} \right)^{-1}. \quad (\text{C2})$$

Using (A1), (B11)

$$\frac{d\gamma_{el}}{dn} = \frac{1}{3} \frac{\gamma_{el}}{n} + \frac{8}{39} \frac{\sigma_T}{m_e c} \xi_B \gamma_{el}^2 \frac{te}{\gamma n}. \quad (C3)$$

To integrate, we need to express  $t$ ,  $e$ , and  $\gamma$  in terms of  $n$ . Let  $\gamma_0$ ,  $n_0$  and  $e_0$  be Lorentz factor, proper density, and proper energy density at the shock passage time  $t_0$ . From (A1), (A3)-(A5),

$$\gamma_0 = \frac{1}{\sqrt{2}} \Gamma_0, \quad (C4)$$

$$n_0 = 2\sqrt{2} \Gamma_0 n_i, \quad (C5)$$

$$e_0 = 2\Gamma_0^2 n_i m_p c^2, \quad (C6)$$

where  $\Gamma_0^2 = T^3/t_0^3$ . From (D8), (A1), (A3)-(A5),

$$\gamma = \gamma_0 (t/t_0)^{-7/2}, \quad (C7)$$

$$n = n_0 (t/t_0)^{-13/2}, \quad (C8)$$

$$e = e_0 (t/t_0)^{-26/3}. \quad (C9)$$

Now (C3) can be written as

$$\frac{d\gamma_{el}}{dn} = \frac{1}{3} \frac{\gamma_{el}}{n} + \frac{8}{39} \frac{\sigma_T}{m_e c} \xi_B \frac{t_0 e_0}{\gamma_0 n_0} \left( \frac{n}{n_0} \right)^{-14/39} \gamma_{el}^2, \quad (C10)$$

and integrated

$$\frac{1}{z} = \frac{1}{z_0} + \frac{4}{19} \frac{\sigma_T}{m_e^2 c^3} \xi_B \xi_e \frac{t_0 e_0^2}{\gamma_0 n_0} (1 - y^{19/6}), \quad (C11)$$

Here  $z \equiv \gamma_{el}/\gamma_e$ , with  $\gamma_e$  defined by (B12),  $y$  is defined by (D1). Plug in (C4)-(C6), express  $\Gamma_0$  in terms of  $a$ ,  $y$ , and  $t_o$ . We get

$$z^{-1} = z_0^{-1} + A(8t_o)^{-1/2} a^{-1} y^{-2} (1 - y^{19/6}), \quad (C12)$$

$A$  is defined by (9),  $a$  is defined by (D2). With the synchrotron cooling given by (C12), the spectral luminosity is

$$L_\omega(t) = 192 \int_0^1 dy y^3 \int_0^1 da a^3 (1 + 7a^2)^{-2} \int dz_0 f_e(z_0) F_0[2a(1 + 7a^2)\omega t_o^{3/2}/z^2]. \quad (C13)$$

#### D. Transverse distances and proper times

Adiabatic lightcurve (B20) is an integral over dimensionless variables  $y$  and  $a$ :

$$y = \frac{\sqrt{2}\gamma}{\Gamma}, \quad (D1)$$

$$ay = (8t_o)^{-1/2}\Gamma^{-4/3}. \quad (\text{D2})$$

To calculate polarization using (B20), we have to express the distance from the observer - burst center line  $h$ , and the proper time since the shock passage  $\tau$ , in terms of  $y$  and  $a$ . This is done here.

The transverse distance is  $h = r\theta$ , and from (A8), (A9)

$$h = \sqrt{2}T\Gamma^{-2/3}(t_o\Gamma^{2/3} - \frac{1}{16\gamma^2})^{1/2}, \quad (\text{D3})$$

and from (D1), (D2)

$$h = \frac{1}{2}T(8t_o)^{5/8}(ay)^{1/4}(1 - a^2)^{1/2}. \quad (\text{D4})$$

Now the proper time... Equation of motion of a shocked particle is

$$\frac{dr}{dt} = 1 - \frac{1}{2\gamma^2} = 8\frac{r}{t} - 7, \quad (\text{D5})$$

here  $t$  is the burst frame coordinate time. Integration gives  $r = t - Ct^8$ . Since the shock front is at

$$R = t - \frac{t^4}{8T^3}, \quad (\text{D6})$$

we get

$$r = t - \frac{t^8}{8T^3t_0^4}, \quad (\text{D7})$$

where  $t_0$  is the burst coordinate time at which the particle was shocked. The similarity variable at the particle is

$$\chi = t^4/t_0^4, \quad (\text{D8})$$

and

$$\tau = \int \frac{dt}{\gamma} = \sqrt{2} \int dt \frac{\chi^{1/2}}{\Gamma} = \frac{2\sqrt{2}}{9T^{3/2}t_0^2}(t^{9/2} - t_0^{9/2}). \quad (\text{D9})$$

Using (D8), (A10), (A7), we get

$$\tau = \frac{2\sqrt{2}}{9}T(8t_o)^{5/8}a^{5/4}y^{1/4}(1 - y^{9/4}). \quad (\text{D10})$$

## E. Degree of Polarization

To estimate the degree of polarization  $\Pi$  we use the adiabatic lightcurve and assume  $F(\omega) \sim \omega^{-s}$  in (B20). The latter simplification should not lead to a large error, because  $\Pi$  turns out to be approximately the same in the relevant range  $1 > s > -1/3$ . With these assumptions, the degree of polarization can be estimated as

$$\Pi = \frac{s+1}{s+5/3} \frac{C_{LL}^{1/2}}{L}. \quad (\text{E1})$$

Here the first factor is polarization of a power-law emission from one patch,  $L$  is the total unpolarized luminosity, and  $C_{LL}$  is the polarized luminosity correlator. Up to an irrelevant factor,

$$L = \frac{1}{4} \int da a^{3-s} (1 + 7a^2)^{-2-s}, \quad (\text{E2})$$

$$C_{LL} = \int da_1 dy_1 da_2 dy_2 (y_1 y_2)^3 (a_1 a_2)^{3-s} [(1 + 7a_1^2)(1 + 7a_2^2)]^{-2-s} C_{12} \min(1, \frac{\epsilon_h \tau}{2\pi h}). \quad (\text{E3})$$

Here the *min*-term comes from the azimuthal angle integral,  $\tau = (\tau_1 + \tau_2)/2$ ,  $h = (h_1 + h_2)/2$ .  $C_{12}$  is the normalized magnetic field correlator, for which we take a simple form corresponding to equations (14),(15).

$$C_{12} = \theta(|\tau_1 - \tau_2| - \epsilon_\tau \tau) \theta(|h_1 - h_2| - \epsilon_h \tau). \quad (\text{E4})$$

We calculated (E1) numerically for different values of  $s$ ,  $\epsilon_h$  and  $\epsilon_\tau$ .

## REFERENCES

- Blandford, R. D., & McKee, C. F. 1976, Phys. Fluids, 19, 1130
- Ginzburg, V. L. 1989, Applications of Electrodynamics in Theoretical Physics and Astrophysics (New York: Gordon & Breach)
- Granot, J., Piran, T., & Sari, R. 1998, astro-ph/9806192
- Katz, J. I., & Piran, T. 1997, ApJ, 490, 772
- Kazimura, Y., Sakai, J. I., Neubert, T., & Bulanov, S. V. 1998, ApJ, 498, L183
- Krall, N. A., 1997, Adv. Space Res., 20, 75
- Loeb, A., & Perna, R. 1998, ApJ 495, L597
- Mészáros, P. & Rees, M. 1997, ApJ, 476, 232
- Paczynski, B. & Rhoads, J. 1993, ApJ, 418, L5
- Piran, T. 1997, in Unsolved Problems In Astrophysics, eds. J. N. Bahcall and J. P. Ostriker (Princeton: Princeton Univ. Press), 343-377
- Reichart, D. E. 1997, ApJ, 485, L57
- Rybicki, G. B., & Lightman, A. P. 1979, Radiative Processes in Astrophysics (New York: Wiley)
- Sagdeev, R. Z. 1966, Rev. Plasma Phys., 4, 23
- Sari, R., Piran, T., & Narayan, R. 1998, ApJ, 497, L17
- Vietri, M. 1997, ApJ, 478, L9

Vietri, M. 1997b, ApJ, 488, L105

Waxman, E. 1997a, ApJ, 485, L5

Waxman, E. 1997b, ApJ, 489, L33

Waxman, E. 1997c, ApJ, 491, L19

Wijers, A. M. J., & Galama, T. J. 1998, submitted to Ap. J. (astro-ph/9805341)

Wijers, A. M. J., Rees, M. J. & Mészáros, P. 1997, MNRAS, 288, L51



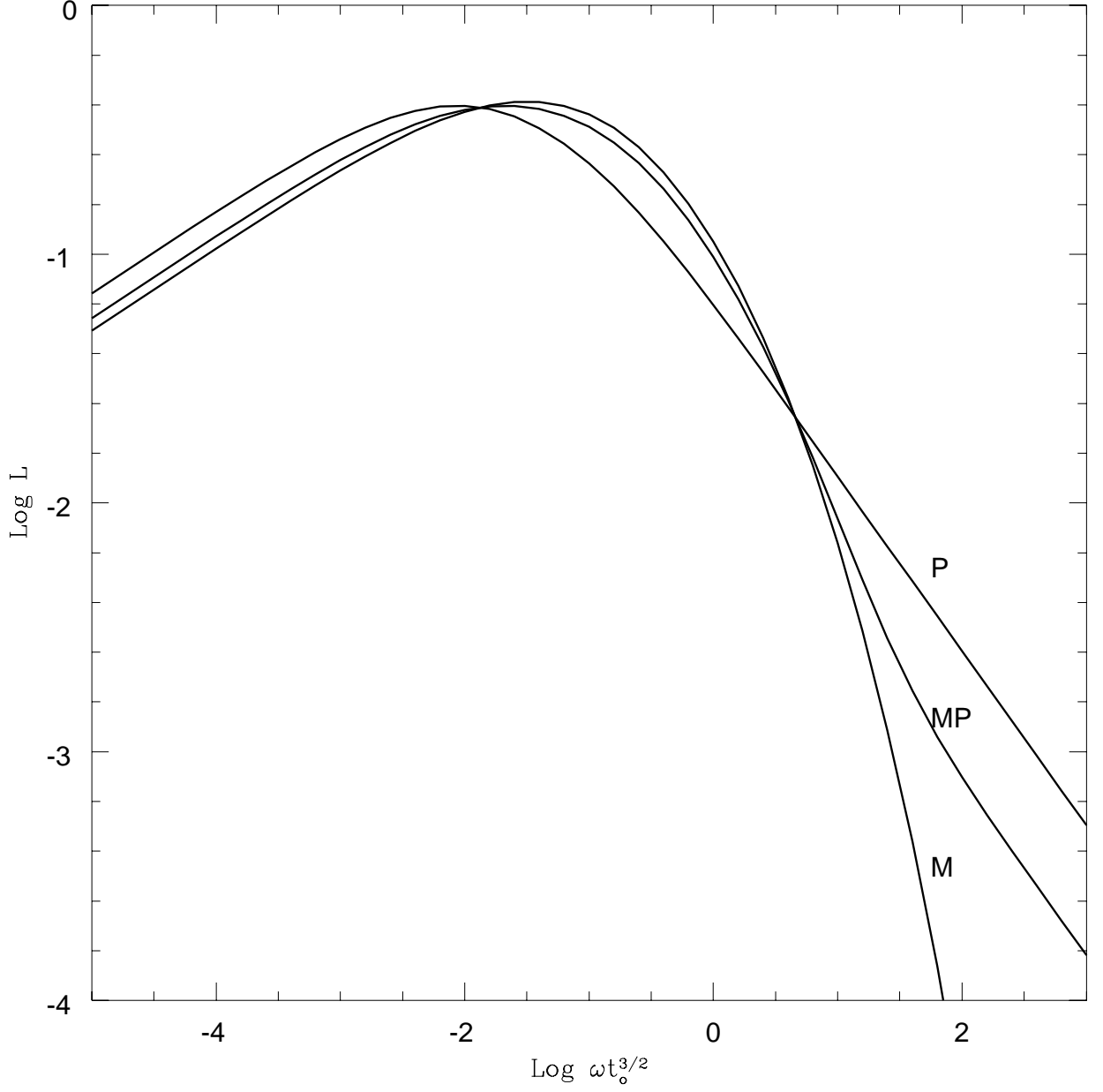


Fig. 1.— Adiabatic lightcurves (6) for different electron distribution functions (§3): power-law P, Maxwellian M, and mixed MP. This graph can be interpreted as luminosity at a given frequency as a function of time, or as the spectrum at a given time.

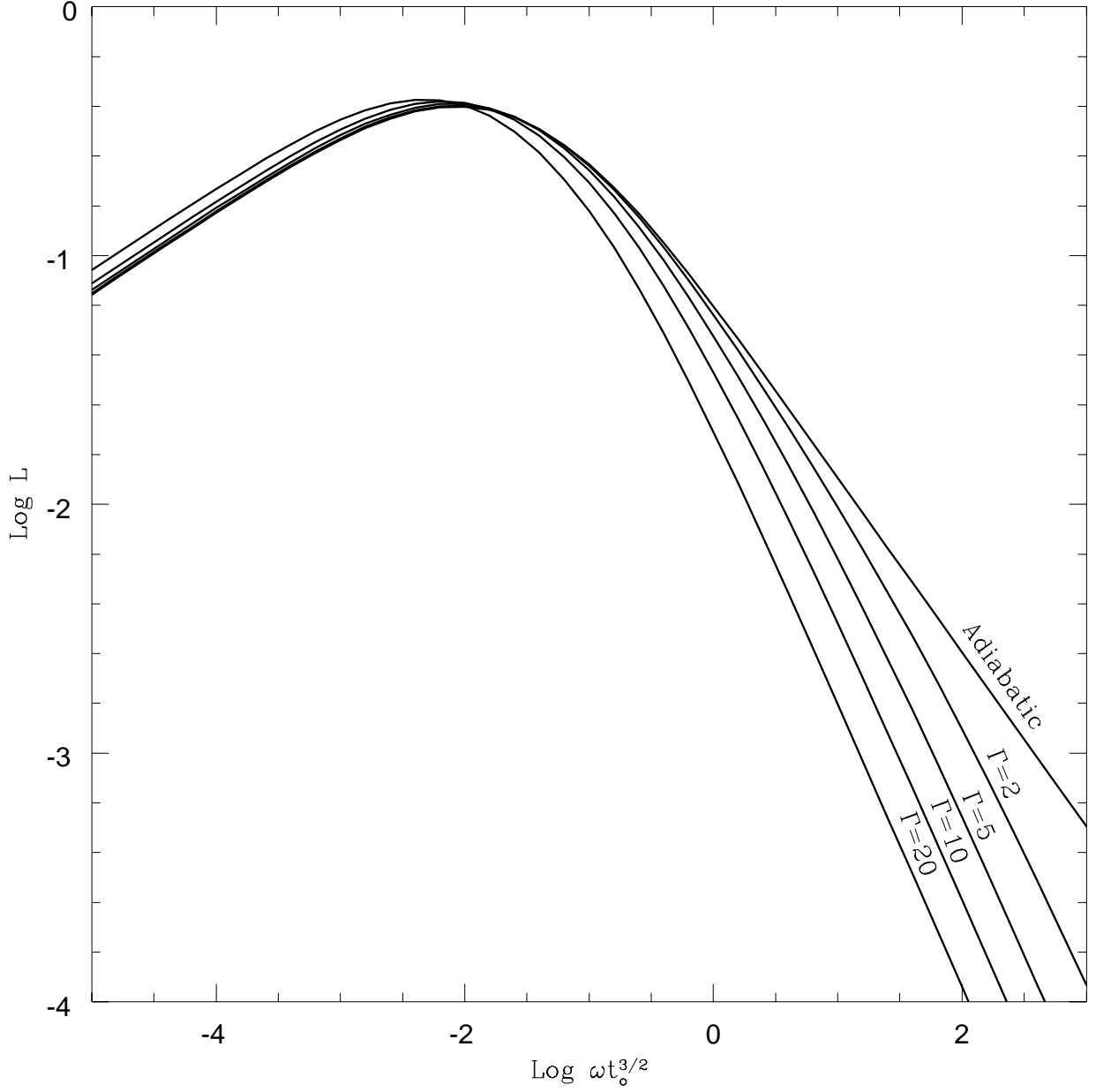


Fig. 2.— Nonadiabatic lightcurves (7) for  $A = 0.01$ , for different observed times, and for a power-law electron distribution function (§3). Adiabatic lightcurve is shown for comparison. Nonadiabatic curves are marked by the Lorentz factors of the shock front at the time when observed photons were emitted from the shock front from  $\theta = 0$ . Observed time in days is  $t_{\text{day}} = 80(E_{52}/n_1)^{1/3}\Gamma^{-8/3}$ .

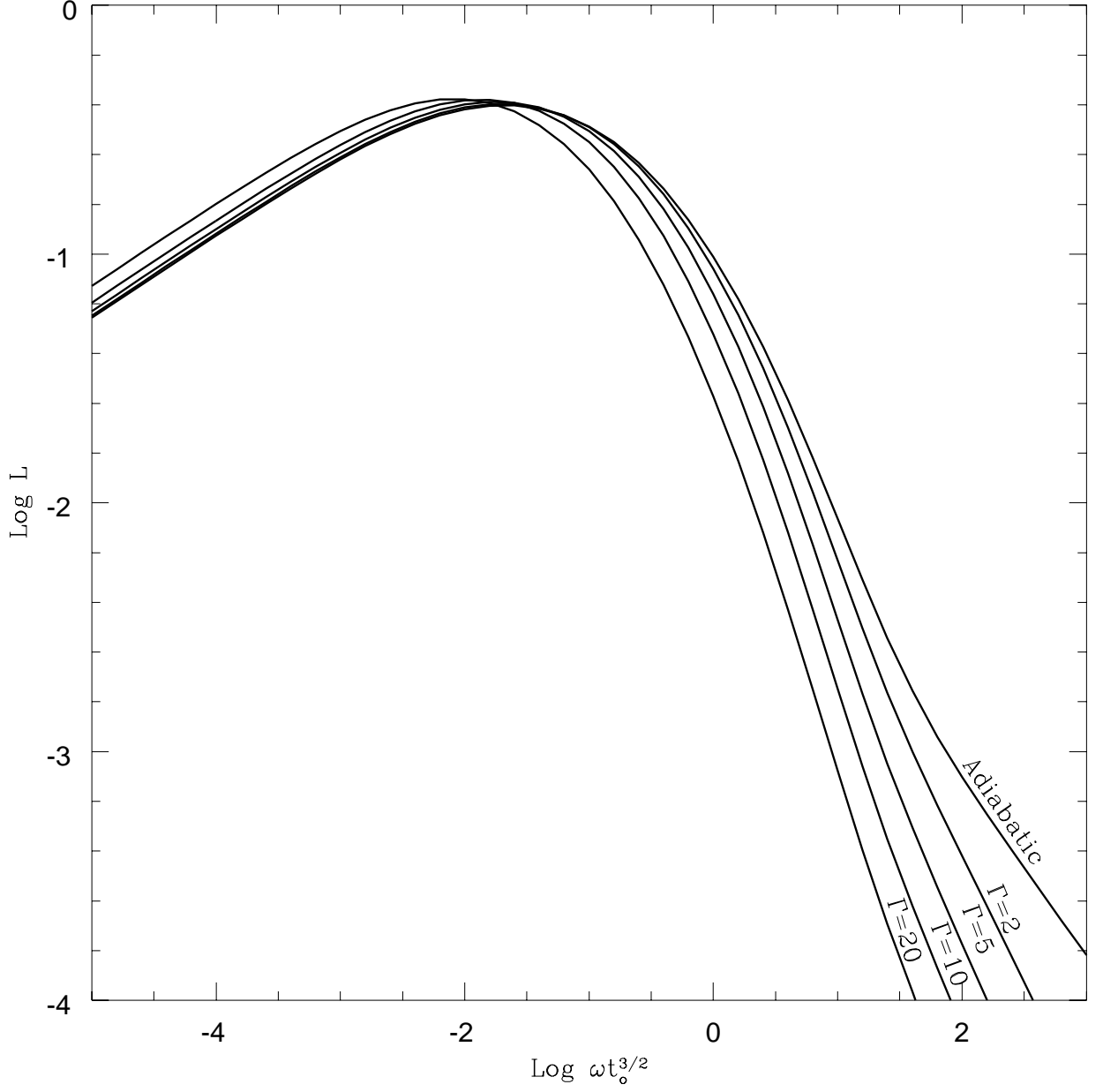


Fig. 3.— Same as Fig. 2, but for the mixed (power-law plus Maxwellian) electron distribution function (§3).